

UDC 541.124.2

(Ba,Sr)TiO₃ - BASED ELECTROLYTE CONDUCTIVITY SENSORS: A COMPARATIVE STUDY

**V.V. Buniatyan², C.A. Huck¹, A.S. Poghossian¹, M.J. Schöning¹,
T.N. Petrosyan²**

¹*FH Aachen | University of Applied Sciences, Institute of Nano- and Biotechnologies, Campus Jülich*

²*State Engineering University of Armenia (Polytechnic)*

A contactless electrolyte conductivity sensor based on **(Ba,Sr)TiO₃ films and Pt** interdigitated electrodes is fabricated and examined. Two types of sensor designs with buried(into insulating SiO₂layer) and non-buried interdigitated electrodes were investigated and compared. The sensors were characterized by means of impedance-spectroscopy measurements indifferent commercially available electrolyte-conductivity standard solutions ranging from 0.084 to 50 *mS/cm* and over the frequency range from 1 *Hz* to 3 *MHz*. It is shown that the parameters of sensors with the Pt electrodes buried in SiO₂ layer are favourable.

Keywords: contactless, electrolyte conductivity, perovskite-oxide film, interdigitated electrode.

Introduction. Chemical sensors and biosensors are becoming more and more indispensable tools in lifescience, medicine, chemistry and biotechnology. Recently, perovskite oxides have aroused increasing attention as catalytically active multifunctional materials in the field of (bio-)chemical sensors. Some of such virgin application frontiers for perovskite oxides of different compositions include, for instance, pH sensing [1-5], hydrogen peroxide [6-8] and hydrocarbon detection [9]. One of the most popular and intensively studied multifunctional perovskite-oxide materials is barium strontium titanate [10]. In previous experiments, the BST films have been applied for the detection of humidity [11-12], hydrogen [13] and ammonia gas [14] or for the development of single sensors sensitive to pH [15,16].

The motivation and description of operation principle of a new type of contactless electrolyte conductivity sensor based on Pt electrodes covered with high dielectric permittivity perovskite-oxide (BST-Barium StrontiumTitanate) nano-films has been examined by us earlier [17-20]. To improve the sensing properties of such sensors we have proposed a new construction, where the interdigitated Pt electrodes are buried in insulating SiO₂ layer.

In the present work, the results of testing of capacitively coupled contactless electrolyte conductivity (C⁴D) sensors with two different electrode designs are

presented. Fig. 1 shows the fabricated C^4D sensor with Pt interdigitated electrodes (IDE) not-buried into the SiO_2 layer. In Fig. 2 the fabricated C^4D sensor with four planar electrodes is presented. The Pt electrodes are buried into the SiO_2 layer to achieve a thinner BST layer thickness and thus a better sensor performance. The fabrication of both sensors' chips is presented and results of testing are compared.

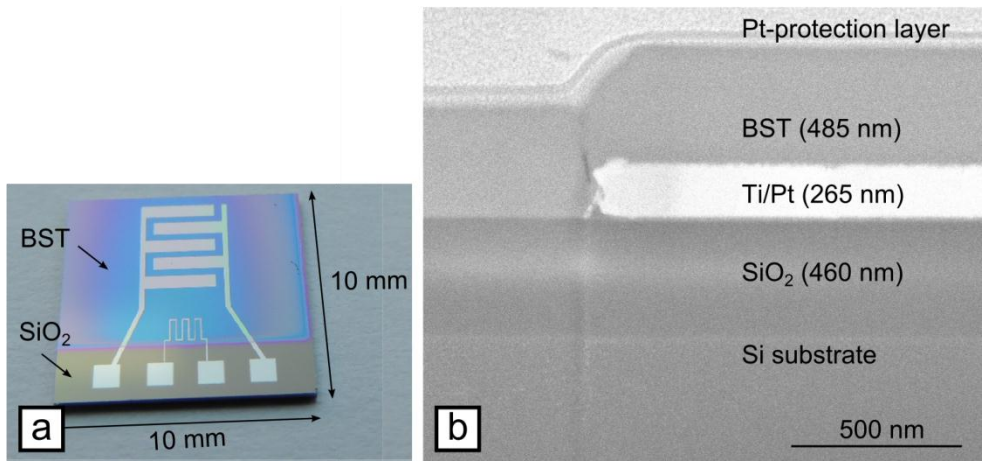


Fig. 1. A photograph of the fabricated C^4D sensor with IDE geometry(a) and cross-sectional SEM image showing the Si- SiO_2 -Ti-Pt-BST layer stack with non-buried electrodes (b)

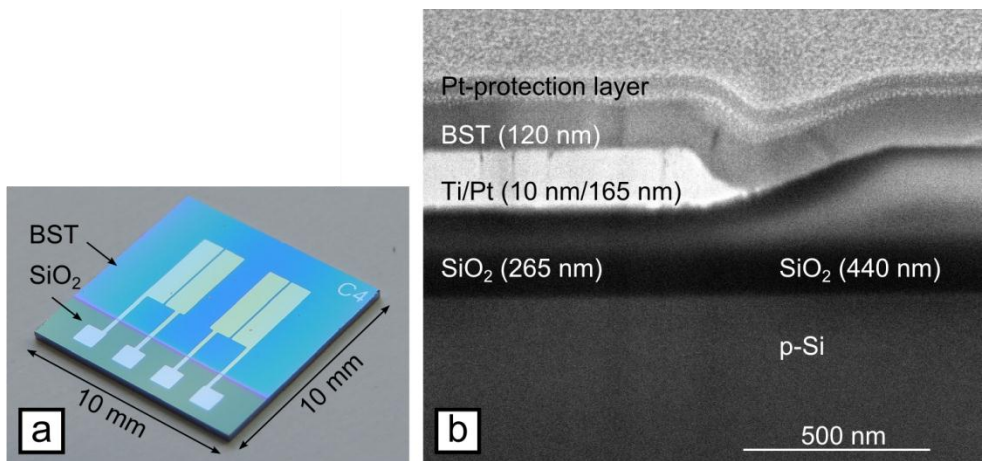


Fig. 2. A photograph of the fabricated C^4D sensor with four electrodes (a) and cross-sectional SEM image showing the Si- SiO_2 -Ti-Pt-BST layer stack with buried Pt electrodes(b)

Fabrication of the sensor chips. Two sensor layouts were fabricated by conventional silicon and thin-film technologies and described in the following. The

first sensor layout includes an IDE structure and is presented in Fig. 3a. Initially, a 440 nm SiO₂ layer was grown by thermal wet oxidation on a silicon substrate (p-Si, $\rho = 1000 \Omega cm$, Topsil Semiconductor Materials, Denmark). In a next step, a thin layer of ~20 nm Ti as adhesion layer and ~200 nm Pt as electrode material were deposited by means of electron-beam evaporation followed by a lift-off process. The geometrical dimensions of the IDE structure are summarized in Fig. 3.

The second sensor layout consists of a four-electrode structure for two- and four-electrode measurements (see Fig. 4). The difference in sensor fabrication is that the electrodes are buried into the SiO₂ substrate. The dimensions of the electrodes and the inter-electrode spacing are summarized in Fig. 4.

Finally, both sensor structures were covered with a protecting BST layer to complete the C⁴D sensors. The BST films of Ba_{0.25}Sr_{0.75}TiO₃ composition were prepared by pulsed-laser deposition (PLD) technique by using targets fabricated via the self-propagating high-temperature synthesis (SHS) method. The process steps of the BST synthesis are described in detail in [15-16]. The BST films were deposited using a Si-shadow mask. The deposition was performed in an oxygen atmosphere (gas flow 30 mL/min, pressure 2x10⁻³ mbar) using a KrF-excimer laser (Lambda LPX305) with a pulse width of 20 ns and a pulse energy of approximately 1J per pulse. When using deposition time of 100 s, energy density of 2.5 Jcm⁻² and repetition rate of 10Hz, the BST layer thickness amounted approximately to 120 nm. Finally, the sensor chips coated with BST were mounted on a printed circuit board (PCB), followed by ultrasonic wire bonding and encapsulation processes.

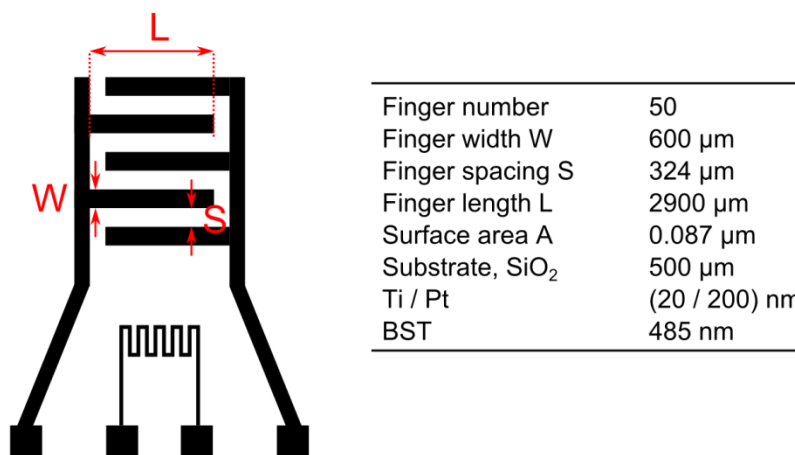


Fig. 3. Layout and dimensions of the interdigitated electrode structure

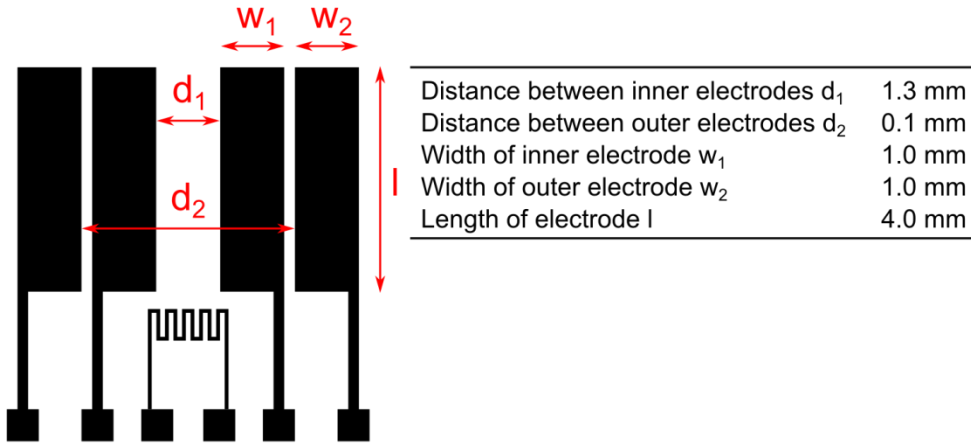


Fig. 4. Electrode arrangement of the fabricated C^4D sensor chip in four-electrode configuration

Characterization of the conductivity sensor. Electrolyte-conductivity measurements are usually conducted using nearly ideally polarized, inert metal electrodes such as platinum or gold, which are in direct contact with the electrolyte. Especially in harsh and aggressive environments, the effect of redox processes, bubble formation due to electrolysis, as well as contamination and fouling of electrodes during continuous use are frequent problems [21-24]. These problems can be overcome, when the electrodes are electrically insulated from the electrolyte solution by covering them with a protective layer [17-24]. The sensor couples capacitively with the electrolyte, which is known as capacitively coupled contactless conductivity detection (C^4D). However, due to the additional capacitance of the protective layer that is usually much lower than the double-layer capacitance of non-protected electrodes, the electrode impedance is increased [22,24,25]. As a consequence, C^4D sensors usually exhibit a lower sensitivity when compared to conventional contact-mode conductivity detection. To find a compromise, the protective material should exhibit a high permittivity in order to reduce the electrode impedance. These requirements are met by the high-k BST thin film.

Both types of electrolyte-conductivity sensors (buried and not-buried) with the protective BST layer were characterized using two-electrode configuration. For characterization, the sensors were exposed to different commercially available electrolyte-conductivity standard solutions ranging from 0.084 to 50 mS/cm . Impedance spectra were recorded with an impedance analyzer (Zennium, ZahnerElektrik GmbH, Germany) covering a frequency range from 1 Hz to 3 MHz. Since electrolyte conductivity is strongly dependent on temperature, all measurements were performed at a constant temperature of 25 °C in a Faraday cage. The conductivity

sensor was calibrated using 12.88 mS/cm and 20 mS/cm conductivity standards, respectively. The impedance spectra (Bode plots) of C⁴D sensors with non-buried and buried electrodes recorded in different electrolyte conductivity solutions are presented in Fig. 4 and Fig. 5, respectively.

Conclusions. As it follows from Fig. 5 and Fig. 6, the characteristic frequency rangewidth of the resistive plateau for the C⁴D sensor with buried electrodes is larger than that of the sensor with non-buried electrodes. The C⁴D sensor with buried electrodes exhibits a wide resistive plateau over more than three frequency decades. This is advantageous because the electrolyte resistance R_{sol} can be measured at a wide frequency range. The obtained results demonstrate the potential of the developed C⁴D sensor with buried Pt electrodes and a BST film as a protective layer for the electrolyte-conductivity measurements in a wide field of applications.

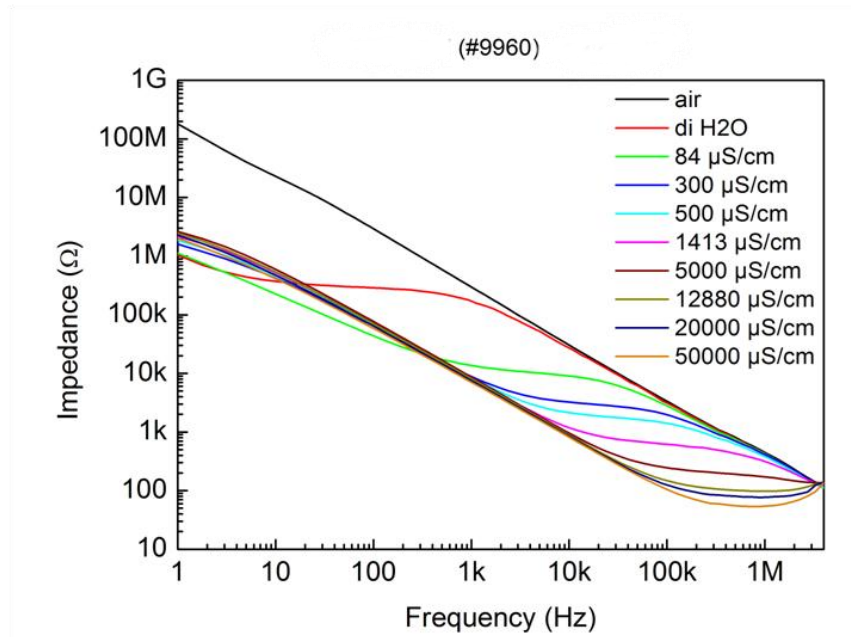


Fig. 5. Bode plots of the C⁴D sensor with non-buried electrodes in two-electrode configuration with 485 nm BST as protective layer recorded in various electrolyte-conductivity standard solutions

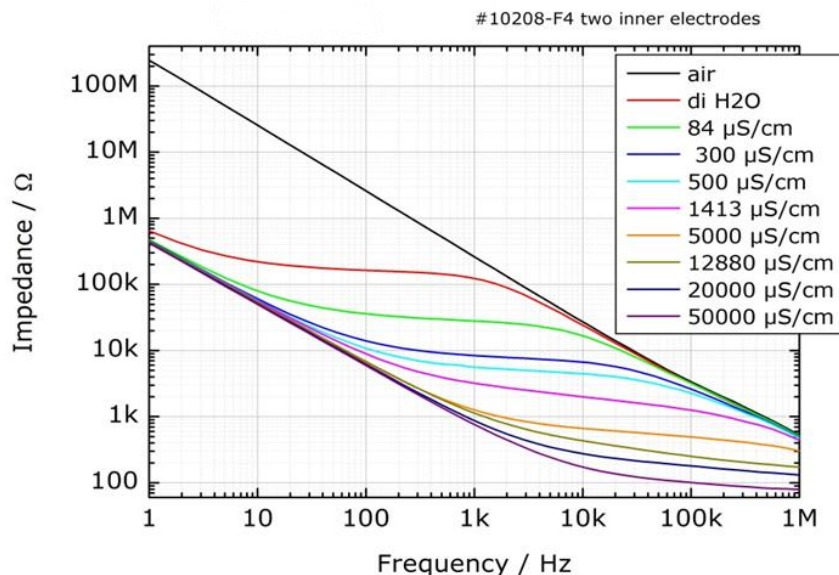


Fig. 6. Bode plot of the C^dD sensor with buried Pt electrodes in two-electrode configuration with 120 nm BST as protective layer recorded in various electrolyte-conductivity standard solutions

Acknowledgments. This work was supported by the State Committee Science MES RA (Grant SCS 13-2G-032) and the European Union (ERDF), “The Commission investing in your future”.

References

1. **Jan S.-S., Chen Y.-C., Chou J.-C.** Effect of Mg^{2+} dopant on the characteristics of lead titanate sensing membrane for ion-sensitive field-effect transistors // Sensors and Actuators B, Chemical. -2005.- 108. - P. 883-887.
2. Design and fabrication of pH detecting system using lead titanate series gate ion-sensitive field effect transistors / **S.-S. Jhan, J.-L. Chiang, Y.-C. Chen, J.-C. Chou, J.-F. Su** // Ferroelectrics.- 2009.- 383. -P. 111-118.
3. **Pan T.-M. , Liao K. -M.** Comparison of structural and sensing characteristics of Pr_2O_3 and $PrTiO_3$ sensing membrane for pH-ISFET application // Sensors and Actuators: B Chemical.- 2008.- 133.- P. 97-104.
4. A new perovskite phase $LiCaTaO$: Li ion conductivity and use as pH sensor / **Q.N. Pham, C. Bohnke, J. Emery, O. Bohnke, F. Le Berre, M.-P. Crosnier-Lopez, J.-L. Fourquet, P. Florian** // Solid State Ionics.-2005.- 176.- P. 495-504.
5. **Roffat M. , Noel O. , Soppera O. , Bohnke O.** Investigation of the perovskite ceramic $Li_{0,30}La_{0,56}TiO_3$ by pulsed force mode AFM for pH sensor application // Sensors and Actuators B: Chemical.- 2009.- 138. - P.193-200.
6. Electrocatalytic activity of perovskite $La_{1-x}Sr_xMnO_3$ towards hydrogen perovskite reduction in alkaline medium / **G. Wang, Y. Bao, Y. Tian, J. Xia, D. Cao** // Journal of Power Sources. -2010.- 195. - P. 6463-6467.

7. Electroless deposition of BaTiO₃nanocubes for electrochemical sensing / **X. He, C. Hu, Y. Xi, B. Wan, C. Xia**: // *Sensors and Actuators B: Chemical*. – 2009.- 137. - P. 62-66.
8. **Luque G.L., Ferreyra N.F., Leyva A.G., Rivas G.A.** Characterization of carbon paste electrodes modified with manganese based perovskites-type oxides from the amperometric determination of hydrogen peroxide // *Sensors and Actuators B: Chemical*.- 2009.-142.- P. 331-336.
9. **Sahner K., Moos R.** Modeling of hydrocarbon sensors based on p-type semiconducting perovskites // *Physical Chemistry Chemical Physics*. -2007.- 9. -P. 635-642.
10. **Zhu W., Tan O.K., Yao X.** Amorphous ferroelectric (Ba_{0,67}Sr_{0,33}Ti_{1,02}O₂) thin films with enhanced H₂ induced interfacial polarization potential // *Journal of Applied Physics*.- 1998.- 84. - P. 5134-5139.
11. **Agarwal S., Sharma G.L., Manchanda R.** Electrical conduction in BaSrTiO₃ thin film MIS capacitor under humid conditions // *Solid State Communications*. – 2001.-119, No.12. - P.681-686.
12. **Agarwal S., Sharma G.L.** Humidity sensing properties (Ba, Sr)TiO₃thin films grown by hydrothermal-electrochemical method // *Sensors and Actuators B: Chemical*.- 2002.- 85.- P.205-211.
13. **Zhu W., Tan O.K., Yan Q., Oh J.T.** Microstructure and hydrogen gas sensitivity of amorphous (Ba, Sr)TiO₃thin film sensors // *Sensors and Actuators B: Chemical*. – 2000.- 65.- P. 366-370.
14. **Roy S.C., Sharma G.L., Bhatnagar M.C., Samanta S.B.** Novel ammonia-sensing phenomena in sol-gel derived Ba_{0,5}Sr_{0,5}TiO₃ thin films // *Sensors and Actuators B: Chemical*.- 2005.-110. - P. 299-302.
15. **Chen C.-Y., Chou J.-C., Chou H.-T., J.** pH sensing of Ba_{0,7}Sr_{0,3}TiO₃/SiO₂ film for metal-oxide-semiconductor and ion-sensitive field-effect transistor devices // *Journal of the Electrochemical Society*. – 2009.- 156. - P. G59-G64.
16. pH-sensitive properties of barium strontium titanate (BST) thin films prepared by pulsed laser deposition technique / **V.V. Buniatyan, M.H. Abouzar, N.W. Martirosyan, J. Schubert, S. Gevorgian, M.J. Schöning, A. Poghossian** // *Physica Status Solidi A*.- 2010.- 207. - P. 824-830.
17. New contactless electrolyte conductivity (EC) sensor / **V.V. Buniatyan, L.G. Rustamyan, H.H. Hovnikyan, et al** // *Proceed. of Engineering Academy of Armenia (PEAA)*. - 2013.- V.10, N3. - P. 531-536.
18. Chemische Sensoren mit Bariumstrontiumtitanat als funktionale Schicht zur Multiparameterdetektion/ **A. Huck, A. Poghossian, M. Backer, et al** // *Proc. of 11th Dresdner Sensor Symposium-2013*. - 2013. - P. 368-372.
19. Equivalent circuit and optimization of impedance characteristics of electrolyte conductivity sensor / **V.V. Buniatyan, C. Huck, A.S. Poghossian et al** // *Proc. of SEUA "Information Technol., Electronics, Radio Engineering"*. - 2014. - Vol. 17, N1. - P. 69-77.
20. Capacitively coupled electrolyte-conductivity sensor based on high-k material of barium strontium titanate / **A. Huck, A. Poghossian, M. Schöning et al** // [Sensors and Actuators B: Chemical](#) v. 198 . - 2014. - Vol. 31. - P. 102–109.
21. **Bousse L., Bergveld P.** On the impedance of the silicon dioxide/electrolyte interface // *Journal of Electroanalytical Chemistry*.- 1983.-152. - P. 25-39.
22. **Rana S., Page H.R., McNeil J.C.** Impedance spectra analysis to characterize interdigitated electrodes as electrochemical sensors // *Electrochimica Acta*.- 2011.- 56.- No.2. - P. 8559-8563.

23. Downscaling aspects of a conductivity detector for application in on-chip capillary electrophoresis / **F. Laugere, G. Lubking, A. Berthoald, G. Bastemeijer, J.M. Vellekoop** // Sensors and Actuators A: Physical. – 2001.- 92, No.1-3. - P. 109-114.
24. **Olthuis W., Volanschi A., Bomer J., Bergveld P.** A new probe for measuring electrolytic conductance // Sensors and Actuators B: Chemical.- 1993.- 13.- P. 230-233.
25. **Olthuis W., Sprenkels A., Bomer J., Bergveld P.** Planar interdigitated electrolyte-conductivity sensors on an insulating substrate covered with Ta₂O₅ // Sensors and Actuators B: Chemical. – 1997.- 43. - P. 211-216.

Received on 17.11.2014.

Accepted for publication on 17.12.2014.

(Ba,Sr)TiO₃ ՀԻՄՔՈՎ ԷԼԵԿՏՐՈԼԻՏԻ ՀԱՂՈՐԴԱԿԱՆՈՒԹՅԱՆ ՉԱՓՄԱՆ ՍԵՆՍՈՐ. ՀԱՄԵՄԱՏԱԿԱՆ ՀԵՏԱՀՈՏՈՒԹՅՈՒՆ

**Վ.Վ. Բունիաթյան, Բ.Ա. Հուկ, Ա.Ս. Պողոսյան, Մ.Ջ. Շյունինգ
Տ.Ն. Պետրոսյան**

Պատրաստվել և հետազոտվել է էլեկտրոլիտի հաղորդականության ոչ հպումային չափման սենսոր՝ հիմնված Pt-ե միկրոմանրակերտ էլեկտրոդների և (Ba,Sr)TiO₃ թաղանթների վրա: Հետազոտվել և համեմատվել են երկու տեսակի սենսորներ՝ Pt-ե միկրոմանրակերտ էլեկտրոդները SiO₂-ի շերտում ընկղմված և չընկղմված: Սենսորները բնութագրվել են իմպեդանս սպեկտրոսկոպիայի մեթոդով ստանդարտ էլեկտրոլիտների՝ 0.084-ից 50 մՍ/սմ հաղորդականությունների և 1 Հց-ից մինչև 3 ՄՀց հաճախությունների համար: Ցույց է տրվել, որ ընկղմված Pt-ե միկրոմանրակերտ էլեկտրոդներով սենսորների պարամետրերը նախընտրելի են:

Առանցքային բաներ. ոչ հպումային, էլեկտրոլիտի հաղորդականություն, պերովսկիթ-օքսիդային թաղանթ, միկրոմանրակերտ էլեկտրոդներ:

ДАТЧИК НА ОСНОВЕ (Ba,Sr)TiO₃ ДЛЯ ИЗМЕРЕНИЯ ПРОВОДИМОСТИ ЭЛЕКТРОЛИТА: СРАВНИТЕЛЬНЫЕ ИССЛЕДОВАНИЯ

**В.В. Буниатян, К.А. Хук, А.С. Погосян, М.Дж. Шенинг,
Т.Н. Петросян**

Изготовлен и исследован датчик для бесконтактного измерения проводимости электролита, основанный на Pt-х микроминиатюрных электродах и на (Ba,Sr)TiO₃ пленках. Изучены и сравнены два вида датчиков: погруженные и непогруженные в слой SiO₂ микроминиатюрные электроды. Датчики характеризуются методом импедансной спектроскопии с использованием стандартных электролитов: проводимостью 0,084 ... 50 мС/см и частотностью 1 Гц ... 3 МГц. Показано, что параметры погруженных датчиков Pt-х микроминиатюрных электродов являются более предпочтительными.

Ключевые слова: бесконтактный, проводимость электролита, перовскит-оксидная пленка, микроминиатюрные электроды.